Zeitschrift: Swiss bulletin für angewandte Geologie = Swiss bulletin pour la géologie appliquée = Swiss bulletin per la geologia applicata = Swiss bulletin for applied geology

Herausgeber: Schweizerische Vereinigung von Energie-Geowissenschaftern; Schweizerische Fachgruppe für Ingenieurgeologie

Band: 29 (2024)

Heft: 1-2

Artikel: The thermo-hydraulics of small water-bearing underground structures

Autor: Siegenthaler, Christoph / Custer, Roland

DOI: https://doi.org/10.5169/seals-1062152

Nutzungsbedingungen

Die ETH-Bibliothek ist die Anbieterin der digitalisierten Zeitschriften auf E-Periodica. Sie besitzt keine Urheberrechte an den Zeitschriften und ist nicht verantwortlich für deren Inhalte. Die Rechte liegen in der Regel bei den Herausgebern beziehungsweise den externen Rechteinhabern. Das Veröffentlichen von Bildern in Print- und Online-Publikationen sowie auf Social Media-Kanälen oder Webseiten ist nur mit vorheriger Genehmigung der Rechteinhaber erlaubt. Mehr erfahren

Conditions d'utilisation

L'ETH Library est le fournisseur des revues numérisées. Elle ne détient aucun droit d'auteur sur les revues et n'est pas responsable de leur contenu. En règle générale, les droits sont détenus par les éditeurs ou les détenteurs de droits externes. La reproduction d'images dans des publications imprimées ou en ligne ainsi que sur des canaux de médias sociaux ou des sites web n'est autorisée qu'avec l'accord préalable des détenteurs des droits. En savoir plus

Terms of use

The ETH Library is the provider of the digitised journals. It does not own any copyrights to the journals and is not responsible for their content. The rights usually lie with the publishers or the external rights holders. Publishing images in print and online publications, as well as on social media channels or websites, is only permitted with the prior consent of the rights holders. Find out more

Download PDF: 09.01.2026

ETH-Bibliothek Zürich, E-Periodica, https://www.e-periodica.ch

The thermo-hydraulics of small water-bearing underground structures

Christoph Siegenthaler[1], Roland Custer[2]

Abstract
Hydraulic and geothermic processes in the underground come more and more into the focus for the prospecting of the geothermal heat flow and for the safety of repositories of dangerous wastes. It is shown that the thermal resistance in the wet domain, the water, is sometimes much lower than in the dry domain, the rock, and is called α-discrepance. It follows that under such circumstances it is virtually the rock which governs the heat transfer. This allows to establish rather simple expressions for the water/rock heat transfers of water bearing fractures or bore holes and allows with some luck an interpretation of thermal springs. The result is shown in graphs for upward and downward flow in tubes, which intend to get a rapid estimation of the expected heat transfers. In the case of thermal springs, the variables F, a shape factor, and of X, the depth of recharge/discharge transition of the water can occasionally be determined. A short digression analyses the energy output of a Hot Dry Rock installation and shows that it turns out that that the energy gain depends primarily on the volume of the fractured domain.

Zusammenfassung.
Hydraulische und geothermische Prozesse im Untergrund rücken immer mehr in den Fokus bei der Prospektion des geothermischen Wärmeflusses und bei der Sicherheit von Endlagern von gefährlichen Abfällen. Es wird gezeigt, dass der Wärmewiderstand im nassen Bereich, dem Wasser, oft viel geringer ist als im trockenen Bereich, dem Gestein, dieser Sachverhalt wird hier als α-Diskrepanz bezeichnet. Daher ist es das Gestein, das die Wärmeübertragung regelt. Dies erlaubt, recht einfache Ausdrücke für die Wasser-Gesteins-Wärmeübertragung von wasserführenden Klüften oder Bohrlöchern zu formulieren und erlaubt bei günstigen Umständen die Tiefe des recharge/discharge Übergangs von Thermalquellen zu bestimmen. Das Ergebnis wird in Diagrammen für die Aufwärts- und Abwärtsströmung in Rohren dargestellt, die eine schnelle Abschätzung der zu erwartenden Wärmeübertragungen ermöglichen. Ein kurzer Exkurs analysiert die Energieausbeute einer Hot-Dry-Rock-Anlage und zeigt, dass der Energiegewinn in erster Linie vom Volumen der geklüfteten Domäne abhängt.

Keywords

Thermo-hydraulics in the underground, heat extraction procedures, thermal springs, HDR applications.

1 Introduction

Hydrothermal underground systems play an important role, be it for energy production, for the safety of underground plants such as repositories for hazardous wastes or for the interpretation of geothermics of springs. The present approach deals with the water of tectonic faults, or faults produced by fracking or for boreholes, i.e., of water ducts with rather small apertures, in contrast to thermic studies of the flow through large porous underground areas (Domenico and Palciauskas 1973, Inagaki and Taniguchi 1994, Sakura 1993, Van der Kamp and Bachu 1989, Anderson 2005). Some properties of the geothermics can be deduced qualitatively, e.g., for a spring (Figure 1):

(**i**) An inspection of the temperature path of a thermal water in the discharge section shows that a water with an extremely large water flux is hardly dependent on the geothermal gradient γ [$\mathrm{K \cdot m^{-1}}$].
(**ii**) The temperature path of an extremely low water flux must follow the thermal gradient.
(**iii**) If X, the length of the discharge section, is large enough, a situation with equal temperature differences between the thermal

1 Zwinglistrasse 40, 8004 Zürich; christoph.siegenthaler@bluewin.ch
2 Müllerstrasse 46, 8004 Zürich; nonius.custer@bluewin.ch

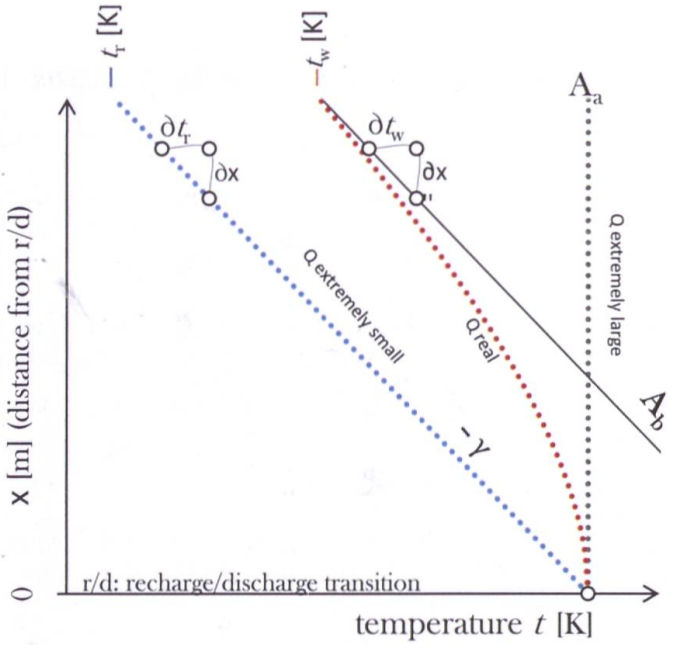

Figure 1. The thermal flow path tw along the discharge section of a thermal well, a qualitative approach. x= distance from the recharge/discharge transition, t_r= rock temperature, Q= water flux. A_a and A_b are asymptotes.

water and the rock is established, i.e., a temperature path which is parallel with the geothermal gradient, avoiding an inflection point of the water path. A water path with an inflection point is regarded as impossible in a homogenous environment with stationary water flows, since Tollmien (1935) states that a hydrodynamic velocity profile with an inflection point is unstable. It is further important to note that the geothermics of water bearing channels can be treated as independent of permeability, as shown by a multitude of detailed studies, e.g., Grigull (1988), and only steady states are examined. The geothermal heat flow, which is in the range of 0.1 [W·m^{-2}], can be neglected for most applications, since thermal springs and technical installations in the underground involve heat flows generally several orders of magnitudes larger than the geothermal heat flow.

2 The variables of the wet domain are often not relevant

The heat transfers in the wet and dry domains are compared with a situation of a water duct bordering a rock with a different temperature. The local heat flow density across the wall and along the flow path x' is

$$q_w'(x') = \mid \alpha_w \cdot (t_{wall}(x') - t_w(x')) \mid [\mathrm{W \cdot m^{-2}}]$$
(Eq.1)

in the wet domain. The convection heat transfer coefficient is $\alpha_w = \mathrm{Nu} \cdot \lambda_w \cdot d^{-1}$ for laminar flow, $d = 4 \cdot A \cdot p^{-1}$ is the hydraulic diameter, A is the cross–sectional area and p is the wetted perimeter of the water duct (Incropera et al. 1990). The Nusselt number Nu is ≈8 for flow between isothermal parallel walls (Edwarts et al. 1979), for flow in tubes it is ≈4 (Eagle et al. 1930 and Jansen 1952), but Nu increases rapidly if turbulences appear. In the dry domain, the mean of the conduction heat transfer coefficient of $\tilde{\alpha}_r$ is

$$\tilde{\alpha}_r = \frac{\lambda_r}{p} \cdot F_{HG}, \quad F_{HG} = \frac{2\pi}{\log_e(\frac{n \cdot X'}{p})}$$
(Eq. 2a, b)

F_{HG} is a shape factor with n = 16 if the body is a thin sheet and is 4π for a column (Hahne et al. 1975). The local heat flow density across the surface of the wall is

$$q_r'(x') = \mid \tilde{\alpha}_r \cdot (t_{r,\infty} - t_{wall}(x')) \mid [\mathrm{W \cdot m^{-2}}]$$
(Eq. 3)

The two local heat flow densities at the wall,

$q_w'(x')$ in the wet domain and $q_r'(x')$ in the dry domain, must be equal. If a large α–discrepance, $\tilde{\alpha}_r << \alpha_w$, exists, the following large inequality,

$$| t_{r,\infty} - t_{wall}(x') | >> | t_{wall}(x') - t_w(x') |$$
(Eq. 4)

leads to $t_w(x') \approx t_{wall}(x')$. In such a case all variables of the wet domain, the Nusselt number, the thermal conductivity of the water, the hydraulic diameter d, and e.g., wall asperities, are considered as not relevant for a geothermal analysis, especially if the water flows in pipe.

It may be noted that a similar result is obtained if the structural thermal resistances of the wet and dry domain, R_w and R_r, are compared. $R_r = (F_{HG} \cdot p \cdot \lambda_r)^{-1}$ [K·W^{-1}] in the dry domain (Hahne et al. 1975) and

$$R_w = \lambda_w^{-1} \cdot \frac{d}{A \,.\, \mathrm{Nu}}$$
(Eq. 5)

in the wet domain (Incropera et al. 1990). $R_w << R_r$ if turbulences occur in the wet domain.

3 Applications of the α–discrepance.

The geothermal heat flow is generally weak, ≈ 0.1 [W·m^{-2}], as compared with the heat flow generated by technical applications in the underground and is therefore neglectable in most cases.

For all examples shown, the value of the thermal conductivity of the rock, λ_r, is 3 [W·m^{-1}·K^{-1}], the diameter of boreholes is 10 cm and the geothermal gradient γ is 0.03 or 0.04 [K·m^{-1}]. The used temperature scale is °C*, which is °C minus 10 °C, the general mean temperature at the earth surface in Switzerland. If a large α–discrepance exists, e.g., several orders of magnitude in the case of fracking, and ≈one order magnitude for bore holes, the thermal energy increment of the water must be equal to the rock/wall heat flow increment, which leads to the simple equation

$$|\partial t_w(x') \cdot Q \cdot c| = | \partial x' \cdot F_{HG} \cdot \lambda_r \cdot (t_w(x') - t_r(x')) | \quad [\mathrm{J \cdot s^{-1}}]$$
(Eq. 6)

x' is the path of the water in the range (0, X'), Q [m^3·s^{-1}] is the water flow and c is the water heat capacity per unit volume, ≈4 [MJ·m^{-3}·K^{-1}]. Equation 6 is now used to solve the heat flow for specific applications.

(**i**) Fractures produced for HDR applications are generally long and have very small apertures, the α–discrepance is therefore extremely large. The geothermal gradient times the depth of the position of the fracture is constant, the solution of equation 6 is

$$\frac{t_r(X) - t_w(x'=0)}{t_r(X) - t_w(x')} = e^{\frac{x' \cdot F_{HG} \cdot \lambda_r}{c \cdot Q}}$$
(Eq. 6a)

The α–discrepance approach leads thus to a simple version as compared with the results of laboratory tests, e.g., the eight formulas summarized by Jiang et al. (2020), and also the results of Li et al. (2017), Ma et al. (2018), He et al. (2019), Luo et al. (2019), Ma et al. (2019) concerning the effects of wall asperities in water bearing fractures. These investigations used small split rock specimens and could therefore not see the great heat transfer dominance of the dry domain.

(**ii**) Heat flow in a vertical borehole with downward water flow, the rock temperature is $\gamma \cdot x$ and the water temperature at the surface is 0 °C*. The temperature profile is, with $Q' = c \cdot Q \cdot \lambda_r^{-1}$ [m],

$$t_w(x) = -\gamma \cdot \frac{Q'}{F_{HG}} + \left(\gamma \cdot \frac{Q'}{F_{HG}} - \gamma \cdot x\right) \cdot e^{-\frac{x \cdot F_{HG}}{Q'}} - \gamma \cdot x$$
(Eq. 6b)

and shown in Figure 2. Equation 6b is important for the analysis of a HDR installation and

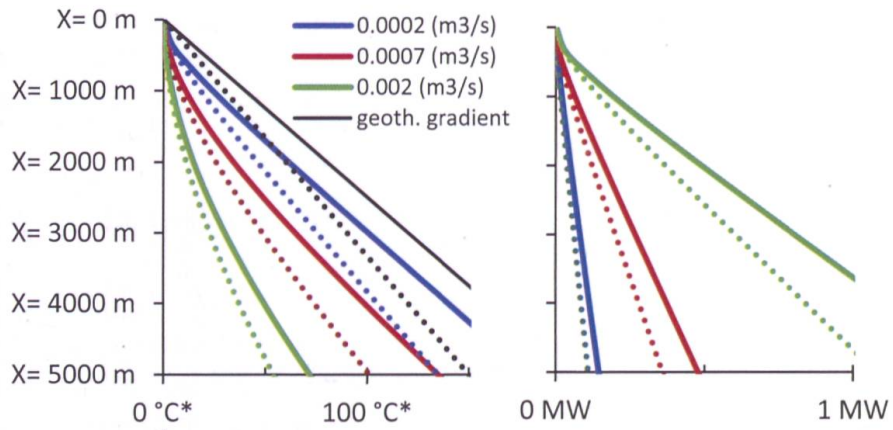

Figure 2a, left: The temperatures of the downward flow in a single vertical borehole, ∅ = 10 cm, which are a function of the thermal gradient γ [K/m] = 0.04 (full line) and γ= 0.03 (stippled line), and of Q [m³·s⁻¹]. X is the length of the borehole; the entrance temperature at the surface is 0 °C*. Figure 2b, right: power gain [MW].

could also be of interest after a borehole had been abandoned because the earthquakes triggered by frackings have been too dangerous, or moving sand had after some time clogged the apertures of fractures, a possibility shown by Benton (2020). In such cases, a second concentric tube for the upward flow of the hot water could possibly be installed, provided an annulus with a high thermal resistance is inserted between the downward and the upward flows to get a warm water spring.

(iii) Upward water flow of underground water. The solution with $t_r(x) = \gamma \cdot (X - x)$ is

$$\Delta t \cdot \gamma^{-1} = Q' \cdot \frac{1 - e^{-\frac{x.F}{Q'}}}{F}, \quad F = \frac{2\pi}{\cos(\beta) \cdot \log_e\left(\frac{16 \cdot X}{p \cdot \cos(\beta)}\right)}$$

(Eq. 6c)

provided that $t_w = t_r$ at $X = 0$; $\Delta t = t_w(x) - t_r(x)$ and F is a shape factor. The Figures 3a and 3b show the temperatures along a vertical tube ($\beta = 0$), e.g., the heat loss of the exploitation of a deep groundwater or of a HDR application.

The equation can 6c also be used for the interpretation of thermal springs if one takes into account that the water path of springs is not always a tectonic fault but may be a +/- large permeable body with a doubtful α–discrepance. Figure 4a shows the thermal springs of northern Switzerland and adjacent regions, a representation which allows to draw any combination of X, the depth of the recharge/discharge transition, and of F, since these two variables are functions of Δt [K]and $Q' = c \cdot Q \cdot \lambda_r^{-1}$ [m]. The interpretation of these data is explained with the three following examples in Figure 4a.

- The thermal spring of Ragaz (green line, Figure 4a) is known for the surprising fact that the water flow Q [m³·s⁻¹] does seasonally largely vary without an expected increase or decrease of the temperature. Sophisticated different water flows had been proposed (Högl 1980), but such effect can be explained by a steep water duct (small shape factor F), a low depth

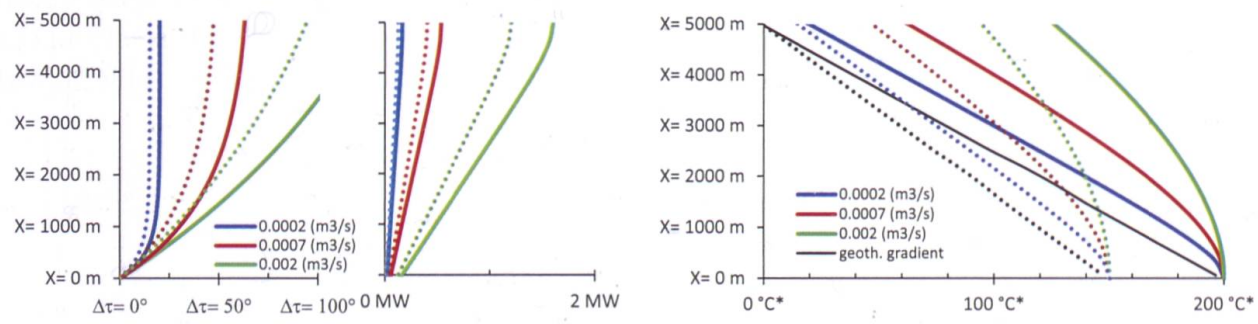

Figures 3a and 3b as Figures 2, but with upward flow, $\Delta t = t_w - t_r$ [0 °C*]. Figure 3c, right Quantitative solution of Figure 1. γ [K/m] = 0.04 (full line) and γ= 0.03 (stippled line).

of the recharge/discharge transition ($X \approx$ 820 m) and a large water flow Q.

- The three springs, blue squares, from very different locations, Black Forest (GE), Yverdon (CH) and Simmental (CH), seem to have similar flow paths and depths, which would lead to F ≈2.2 and to X ≈5000 m; the thermal spring paths could be transcurrent faults.
- Long-term variations of Q and Δt of a spring allows to determine the two variables X and F. Or neighbouring springs could have similar depth X and similar shape factors, e.g., the springs near the positive Waldshut heat dome, marked by red dots, which would lead to X =1600 m and F= 8 (Figure 4a); such an interpretation implies an improbable flat flow path, Figure 4b, and the assumed common X and F is thus obviously wrong.

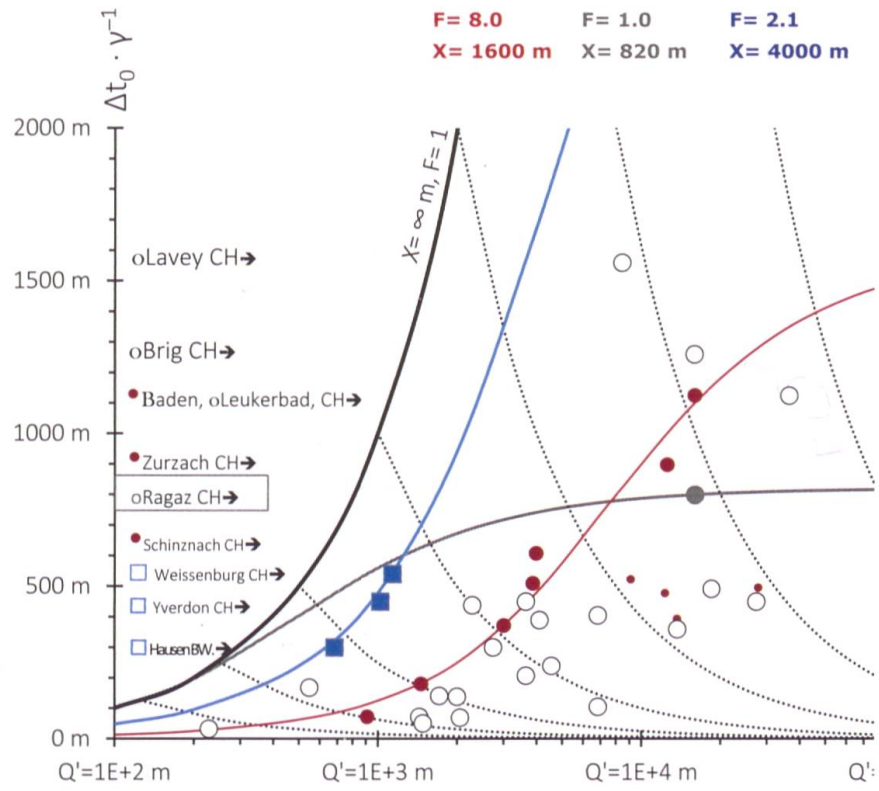

Figure 4a. Thermal springs in and around Switzerland. Stippled lines: path of a thermal spring contaminated by surficial water. Blue squares: samples from three different regions; red dots: springs at or near the Waldshut positive geothermal heat dome (small red dots: springs probably contaminated by surficial water); green dot: the spring of Ragaz. Shown are the F and X interpretation of the three samples. X is the depth of the recharge /discharge transition of a thermal spring.

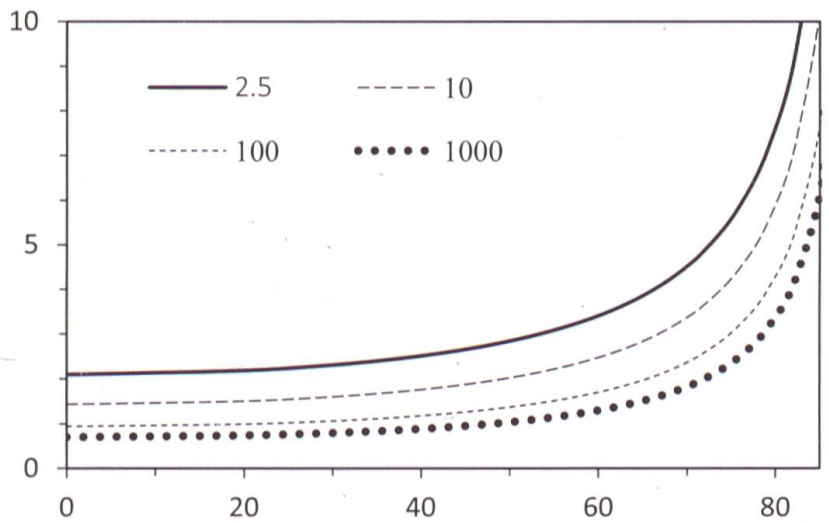

Figure 4b: The shape factor F is a function of the angle ß, the deviation from the vertical, and of X/p, p is the wetted perimeter of the water duct.

4 The Hot Dry Rock energy gain.

The HDR technique draws heat from the deep underground with two boreholes. An essential element of this technique is a permeable body created by an intensive fracking process. This body is now assumed to be a sphere with radius r_1 to simplify the analysis. The involved heat flows around this sphere at the depth X are, for steady state, $q_{out} = q_{in} + q_{rock} + q_{earth}$ [W], shown in Figure 5a, leading to the equation

$$c \cdot Q\, t_{out} = c \cdot Q \cdot t_{in} + 4 \cdot \pi \cdot r_1 \cdot \lambda_r \cdot (\gamma \cdot X - t_{out}) + \pi \cdot \lambda_r \cdot \gamma \cdot r_1^2 \text{ [W]}$$

(Eq. 7)

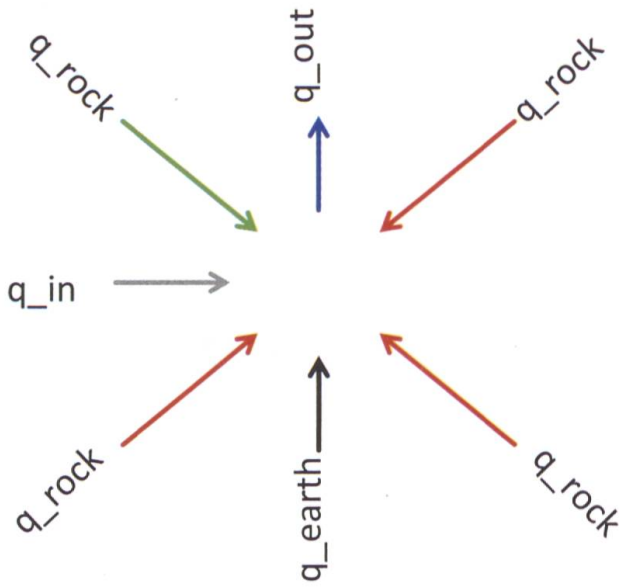

Figure 5a. Schematic view of the relevant HDR thermal flows at depth X, the steady state with the spherical fractured body (blue, with radius r_1), and the relevant heat flows q_in, q_rock, q_earth, and q_out.

$t_{in}(X)$ is the water temperature given in Figure 2a, c [J·m^{-3}·K^{-1}] is the heat capacity per unit volume of water. The second term on the right–hand side is from Hahne and Grigull (1975), the last term is the contribution of the geothermal heat–flow.
It follows from Equation 7 that t_{out}/t_{in} is ≈1 for small values of r_1, and rises up to ≈1.2 for r_1 = 50 m; the thermal power at the surface is therefore negative for steady state.

The total energy gain from the fractured sphere with radius r_1 is the original thermal energy of the sphere minus the remaining energy at the steady state,

$$q_1' = 4/3 \cdot \pi \cdot r_1^3 \cdot c \cdot (\gamma \cdot X - t_{out}) \text{ [J]}$$

(Eq. 8)

shown in Figure 5b for two different depths X, 2118 m (thin stippled lines) and 4206 m (thin full lines), and for different water flows; the geothermal flow is 0.04 [K·m^{-1}].

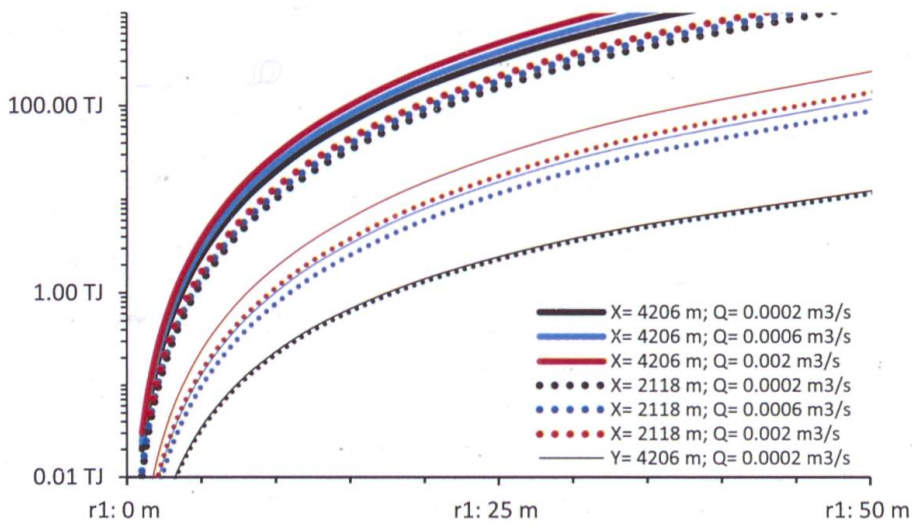

Figure 5b. The total energy yield expected during the operation of a HDR installation. This energy is a function of the radius r_1 of the spherical fractured body, of the involved water flow and of X, the depth. The fine lined group represents the energy from the fractured body, the coarse lined group the energy from outside the fractured body. At depths X=2118 m, stippled lines, and X= 4206 m, full lines.

Outside the fractured sphere, the heat flow after a HDR installation will be very high at the beginning of the operations and will decrease with time until a steady state is attained, this state is described by Hahne and Grigull (1975) with two different formulas,

$q_2 = 4 \cdot \pi \cdot r_1 \cdot \lambda_r \cdot (\gamma \cdot X - t_{out})$ and $q_2 = 4 \cdot \pi \cdot \lambda_r \cdot (\gamma \cdot X - t_2) / (1/r_1 - 1/r_2)$ [W]
(Eq. 9a, b)

The second formula operates with a second concentric sphere, ◎, with radius $r_2 > r_1$ and a temperature t_2 at r_2. Combining the two equations leads to

$r_2 / r_1 = (\gamma \cdot X - t_{out}) / (t_2 - t_{out})$
(Eq. 9c)

for steady state. It is not expected that the HDR operation will last until a steady state is appearing with a negative thermal power. This implies that t_2 is expected to be less than $\gamma \cdot X$, and it is guessed that t_2 could be around $\gamma \cdot X \cdot 0.75$, with $r_2 = 2 \cdot r_1$. The total energy output, q²', from outside the fractured body is then around

$q_2' = 4/3 \cdot \pi \cdot c \cdot (r_2^3 \cdot \gamma \cdot X - r_1^3 \cdot t_{out})$ [J]
(Eq. 10)

shown in Figure 5b (coarse lines). The two energies, equation 8 and 10, presuppose a downstream water temperature of °C*=0, which is °C minus 10° C, the mean temperature at the surface in Switzerland; the heat losses of the upstream flow to the surface have been neglected.
It is important to point out that geothermal heat-flow is not taken into account in the present analysis. According to equation 9a, the geothermal power is very low at the start of operation and is 3 kW at the end of operation with a radius of the fractured body of r = 1 m at a depth of 2118 m, for r = 52 m the power is 165 kW. At a depth of 4206 m the power is 6 kW and 328 kW for r= 1 m and r= 52 m respectively.

5 Conclusion.

A large α–discrepance allows to neglect the variable of the wet domain; the thermo–hydraulics is then drastically simplified in such cases and allows to estimate analytically the heat flows of water bearing structures in the underground. An undoubted α–discrepance does occur for structures generated by hydraulic fracture and does contradict the results of laboratory tests; these investigations used small split rock specimens and could therefore not see the dominance of the thermal resistance of the rock.

A short insertion deals with the energy gain of HDR installations, it turns out that substantial energy gains are only expected if large fractured areas exist.

Finally, the authors want to stress the point that the present analysis is largely based upon the work of Hahne and Grigull (1975), a heat flow catalog of the steady states of around fifty different geometrical configurations embedded in a homogeneous environment.

Acknowledgements

The authors are grateful to Elco Luijendijk for his comments on the first version, his detailed propositions have substantially improved our geothermal descriptions. Many thanks go also to his colleague, Jonas Kley, but we did not want to consider his request that first we had to show that an analytical approach is still justified today. And last but not least great gratitude to Isabelle Fassbind for here readiness to discuss any detail of this paper.

References

Anderson, MP. 2005: Heat as a groundwater tracer. — Groundwater 43/6, p. 951-968.

Benton, DJ. 2020: Particle tracking in porous media with directed fractures. http://dudleybenton.altervista.org/projects/Fractures/index.html.

Domenico, PA. & Palciauskas, VV. 1973: Theoretical analysis of forced convective heat transfer in regional ground-water flow. — Geol. Soc. Amer. Bull. 84, p. 3803-3014.

Eagle, A. & Ferguson, MN. 1930: On the coefficient of heat transfer from the internal surface of tube walls. Proc. Roy. Soc. (A) 127, p. 540-566.

Edwards, DK., Denny, VE. & Mills, AF. 1979: Transfer Processes. 2nd ed. Hemisphere, Washington D.C.

Grigull, U. 1988: Die Grundgesetze der Wärmeübertragung. — Springer Berlin, 3rd edition, 436 p.

Hahne, E. & Grigull, U. 1975: Formfaktor und Formwiderstand der stationären mehrdimensionalen Wärmeleitung. — Int. J. Heat Mass Transfer, 18: 751-767.

Högl, O. 1980: Beschreibung und Analyse der einzelnen Mineralquellen der Schweiz. — In Högl, O (ed.): Die Mineral- und Heilquellen der Schweiz. — Bern und Stuttgart (Paul Haupt): 145–296.

Griesser, JC. & Rybach, L. 1989: Numerical Thermohydraulic Modeling of Deep Groundwater Circulation in Crystalline Basement: An Example of Calibration. — In: AE Beck, G. Garven & L. Stegena (eds.): Geophysical Monograph Series; Hydrogeological Regimes, v. 47, p. 65-74.

He, R., Rong, G., Tan, J. & Cheng, L. 2019: Numerical investigation of fracture morphology effect on the heat transfer characteristics of water flow through a single fracture. Geothermics, v. 82, p. 51-62.

Inagaki, N. & Taniguchi, M. 1994: Estimations of hydraulic conductivity and groundwater flow systems by using groundwater temperature in Nara Basin Japan. — Journal Japanese Assoc. Hydrolog. Sci. 24/3, p. 171-182.

Incropera, PI. & DeWitt, DP. 1990: Fundamentals of Heat and Mass Transfer. — 3rd edition. John Wiley Sons.

Jansen, L. 1925: Zum Wärmeübergang bei laminarer Strömung zwischen parallelen Platten. Schweiz. Bauzeitung 70, p. 535-536.

Jiang, Y., Yao, H., Cui, Y., Lei, H., He, Y. & Bai, B. 2020: Evaluative analysis of formulas of heat transfer coefficient of rock fracture. Int. J. Thermophysics 41, p. 104-120.

Li, Z., Feng, X., Zhang, Y., Zhang, C., Xu, T. & Wang, Y. 2017: Experimental research on the convection heat transfer characteristics of distilled water in manmade smooth and rough rock fractures. Energy, 133: 206-218.

Luo, Y., Xu, W., Lei, Y., Wu, P., Qin, G. & Ba, R. 2019: Experimental study of heat transfer by water flowing through smooth and rough rock fractures. Energy Reports, 5: 1025-1029.

Ma, Y., Zhang, Y., Yu, Z., Huang, Y. & Zhang, C. 2018; Heat transfer by water flowing through rough fractures and distribution of local heat transfer coefficient along the flow direction. International Journal of Heat and Mass Transfer, 119: 139-147.

Ma, Y., Zhang, Y., Hu, Z., Yu, Z., Huang, Y. & Zhang, C. 2019: Experimental study of the heat transfer by water in rough fractures and the effect of fracture surface roughness on the heat transfer characteristics. Geothermics, 81: 235-242.

Sakura, Y. 1993: Groundwater flow estimated from temperatures in the Yonezawa Basin, Northest Japan. — Tracers in Hydrology, IAHS Publication 215, p. 161-170.

Tollmien, W. 1935: Ein allgemeines Kriterium der Instabilität laminarer Geschwindigkeitsverteilungen Nachr. Ges. Wiss. Göttingen, math. Phys. Kl. Fachgr. I1, p. 79-114. Translation in NACA Techn. Mem. Nr. 792, 136.

Van der Kamp, G. & Bachu, S. 1989: Use of dimensional analysis in the study of thermal effects of various hydrogeological regimes. — In: AE Beck, G. Garven & L. Stegena (eds.): Hydrogeological Regimes and Their Subsurface Thermal Effects. — Geophysical Monograph 47; IUGG vol. 2, American Geophysical Union, Washington, D.C.: p. 23-28.

Variables

A	[m^2] Cross–sectional area
c	≈4 [$MJ \cdot m^{-3} \cdot K^{-1}$] Water heat capacity per unit volume
d	[m] Hydraulic diameter $4 \cdot A \cdot p^{-1}$
F_{HG}	[-] Shape factor
Nu	Nusselt number
p	[m] Wetted perimeter of the water duct
r_1	[m] Radius of the spherical fractured body
r_2	[m] Radius of the spherical body $r_2 > r_1$
R	[$m \cdot K \cdot W^{-1}$] Thermal resistance
$q(x')$	[$W \cdot m^{-2}$] Local heat flow density
Q	[$m^3 \cdot s^{-1}$] Water flow
Q'	[m] $c \cdot Q \cdot \lambda_r^{-1}$
t	[K] Temperature
W	[Watt], Geothermal power
X, X'	[m] Vertical or oblique length or depths
x, x'	[m] $0 \le x \le X$; $0 \le x' \le X'$
α	[$W \cdot m^{-2} \cdot K^{-1}$] Conduction heat transfer coefficient
$\tilde{\alpha}_r$	[$W \cdot m^{-2} \cdot K^{-1}$] Rock conduction heat transfer coefficient
ß	Angle, deviation from the vertical
γ	[$K \cdot m^{-1}$] Geothermal gradient, = 0.03 or 0.04
λ	[$W \cdot m^{-1} \cdot K^{-1}$] Thermal conductivity. λ_r, ≈3

Subscripts

r	rock
w	water
wall	wall of tube